13th World Conference on Earthquake Engineering
Vancouver, B.C., Canada
August 1-6, 2004
Paper No. 363

PROPOSAL FOR THE NEW SHEAR RESISTANT MECHANISM AND ITS ULTIMATE SHEAR STRENGTH OF RC BEAM

Setsurou NOMURA[1], Tomohisa MUKAI[2], Tadashi KAJIWARA[3], Takahiro WATANABE[4]

SUMMARY

This paper deals with the ultimate shear strength of reinforced concrete beam with sufficient shear reinforcement, where the shear reinforcement does not yield. The experimental results showed the different values from the calculation ones given by the truss-strut model. It is thought that three dimensional deformation of core concrete should be considered when shear reinforcement does not yield. Several specimens with sufficient reinforcement were tested under monotonic loading, and the strength deterioration relationships of core concrete were examined. The deformation of core concrete was calculated by the strain and the curvature of shear reinforcement. It is found that the expanding deformation of core concrete causes the degrading shear resistant mechanism. As a result, new shear resistant mechanism is proposed by quantifying the expansion behavior of core concrete.

INTRODUCTION

In the Design Guidelines for Earthquake Resistant Reinforced Concrete Buildings Based on Inelastic

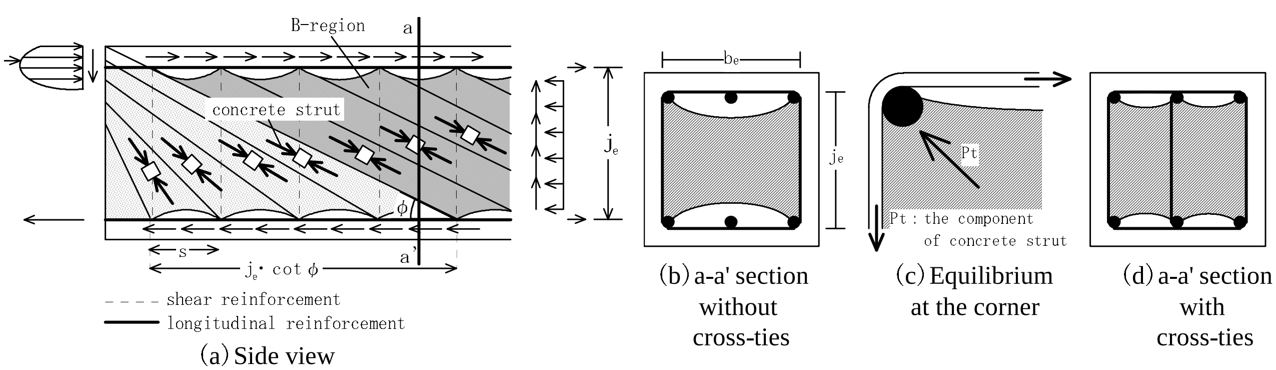

Fig.1 Compressive stress field

---

[1] Department of Architecture, Tokyo Univ. of Science, Noda-city, JAPAN. nomura@rs.noda.tus.ac.jp
[2] Department of Architecture, Tokyo Univ. of Science, Noda-city, JAPAN. mukai@rs.noda.tus.ac.jp
[3] Department of Architecture, Tokyo Univ. of Science, Noda-city, JAPAN. j7103616@ed.noda.tus.ac.jp
[4] TODA CORPORATION, JAPAN

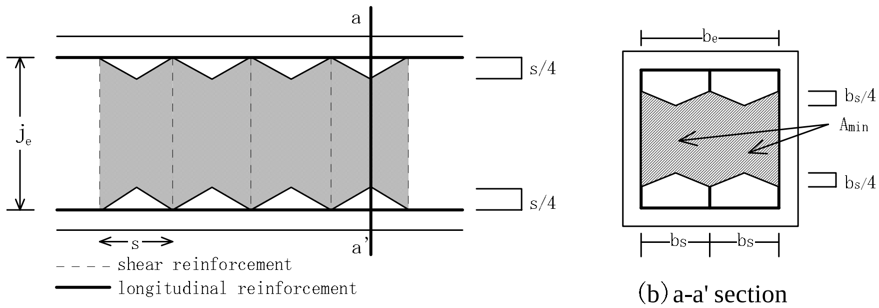

(a) Side view

(b) a-a' section with cross-ties

Fig.2 Simplified stress field

Displacement Concept (1999) [1], the shear strength of RC beams are calculated by the truss-strut model, where the compressive stress field is defined as Fig.1. The minimum effective area at the center of hoop spacing, A_{min} in Fig.1 (b), is given by the Eq.1 with simplifying as seen in Fig.2 (b):

$$A_{min} = \left(1 - \frac{s}{2j_e} - \frac{b_s}{4j_e}\right) \cdot b_e j_e = \lambda \cdot b_e j_e \tag{1}$$

where s and b_s are longitudinal and transverse spacing of hoops shown as Fig.2(a),(b), b_e and j_e are width and depth of core concrete(center-to-center distance of peripheral shear reinforcement) as Fig1(b). When the specimen does not fail in flexure, and when the shear reinforcement does not yield, the shear failure is caused by compressive failure of core concrete. Therefore, the shear strength is expressed as a function of the concrete strength (Eq.(2)).

$$V_u = \frac{\nu \sigma_B}{2} A_{min} \tag{2}$$

where σ_B is compressive strength of concrete, and ν is an effectiveness factor for concrete strength defined by Eq.(3).

$$\nu = 0.7 - \frac{\sigma_B}{200} \tag{3}$$

However, previous experimental results [2] shows that the shear strength cannot be predicted accurately by Eq.(2). Ichinose insisted that three dimensional deformation of core concrete should be considered when shear reinforcement does not yield from result of analytical investigation[3]. In past study, monotonic loading tests on RC beams with sufficient shear reinforcement focusing on the behavior of core concrete were conducted by the authors, and it is found that the expansive behavior of core concrete causes the degrading shear resistant mechanism.

In this paper, several specimens were tested under statically loading, and the relation between the ultimate strength and deformation of core concrete was investigated. Three different shaped specimens with sufficient reinforcement were tested under monotonic loading, and the relationship between the strength deterioration and deformation of core concrete were examined. The deformation of core concrete was calculated by the strain and the curvature of shear reinforcement. To compare the effect of loading excursion on shear resistant mechanism, one specimen with sufficient reinforcement was tested under reversal cyclic lateral loading. Three specimens with different reinforcement bar sections were tested where the sectional areas are same (round, two types of rectangular), but geometrical moment of inertias are different. As a result, new shear resistant mechanism to RC beam with sufficient shear reinforcement is proposed by quantifying the expansion behavior of core concrete.

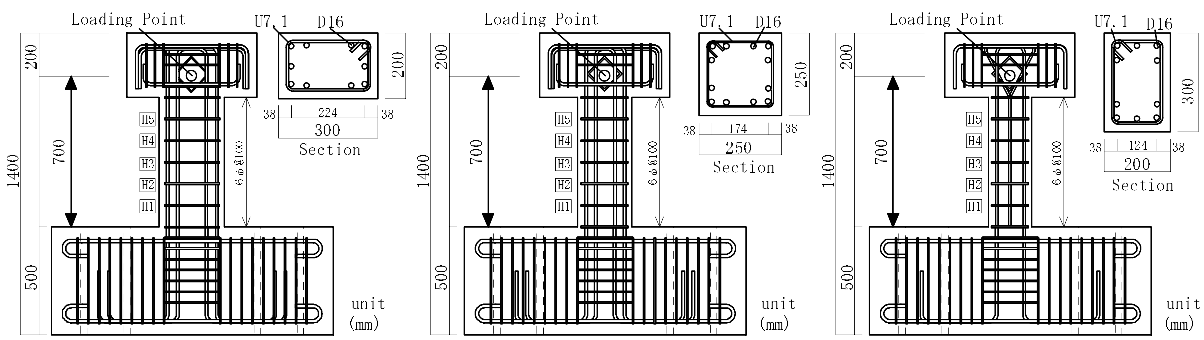

(a) Specimen-A (b) Specimen-B (c) Specimen-C

Fig.3 Geometry and reinforcement details

Table 1 Material properties

(a) Steel

	Yield Strength (N/mm^2)	Yield Strain ($\times 10^{-6}$)	Young's Modulus (N/mm^2)
Specimen-E	814	4451	2.10×10^5
Specimen-F	796	4078	2.12×10^5
Specimen-G	728	3841	2.13×10^5

(b) Concrete

Specimen	E	F	G
Concrete Strength (N/mm^2)	19.8	19.7	20.1

SHEAR BENDING MONOTONIC LOADING TESTS ON DIFFERENT SHAPED SPECIMENS

Outline

The details of specimens are shown in Fig.3, material properties are listed in Table 1, and test setup is shown in Fig.4. The specimen-B, C had different sectional shape but same sectional area of specimen-A. All these specimens have same shear span ratio, 2.3, and ratio of shear reinforcing bar, 0.4%, and tensile reinforcement ratio, 1.7%. The high strength steels listed in Table 1 are used for the shear and longitudinal reinforcement of all specimens in order to lead to the shear failure caused by compressive failure of core concrete. These specimens were tested under monotonic loading, and the drift angle R defined in Fig.4 is calculated from the measurement of the pinned loading point. The strain and curvature of shear reinforcement were measured in the each transverse section of specimens from H1 to H5 (Fig.3), using strain gauges attached as shown in Fig.5.

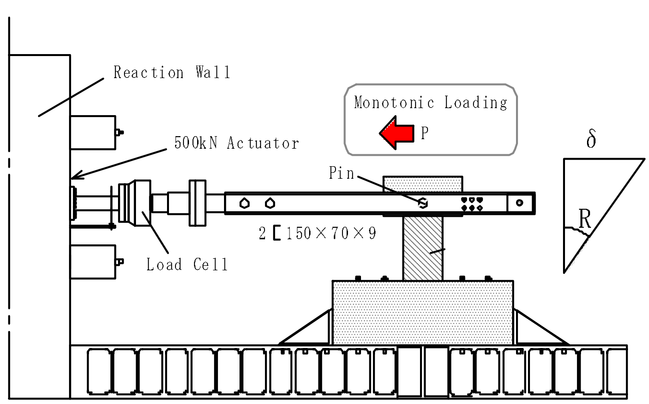

Fig.4 Test setup

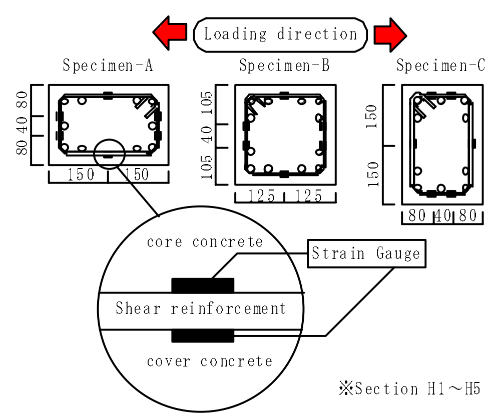

Fig.5 Strain gauge pasted on shear reinforcement

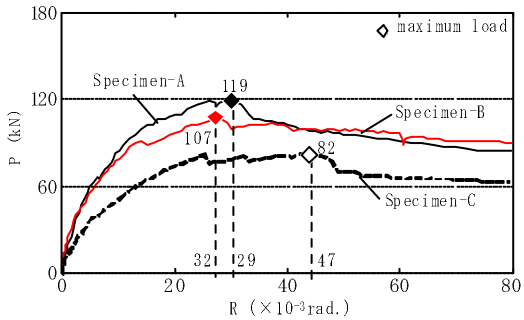

Fig.6 Load P -Drift angle R relationship

Table 2 Maximum strength

Specimen		A	B	C
Experiment (kN)	V_{max}	119	107	82
Calculation (kN)	V_{cal}	137	114	53
V_{max}/V_{cal}		0.87	0.94	1.54

Result and investigation

The observed load P- drift angle R (P-R) relationships for specimens are shown in Fig.6, and the comparison of experimental values with calculation (Eq.(2)) ones are listed in Table 2. All specimens failed in shear, and the strength deterioration occurred when angle R reached to 32×10^{-3}rad.(specimen-A), 29×10^{-3}rad.(specimen-B), 47×10^{-3}rad.(specimen-C) as shown in Fig.6. The shear strength of specimen-A is higher than other specimens. Eq.(2) slightly overestimates the shear strength of specimen-A, B, but it exceedingly underestimate that of specimen-C.

To investigate the relationship between the strength deterioration and the behavior of core concrete, the incremental area of core concrete is assumed to be estimated by the following method.

The increment of sectional area consists of the expanding areas caused by those calculated deformations as the flexural bending and the axial elongation of shear reinforcement as shown in Fig.7. As shown in Fig.8, the curvature φ and axial strain ε_L of shear reinforcement can be described as Eq.(4) and Eq.(5).

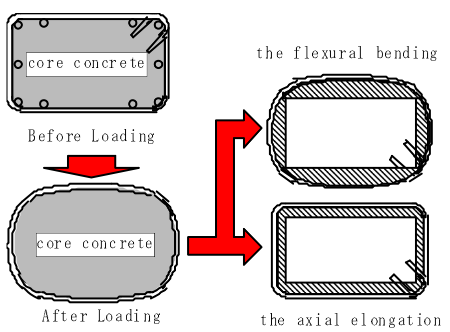

Fig.7 Sectional area of core concrete

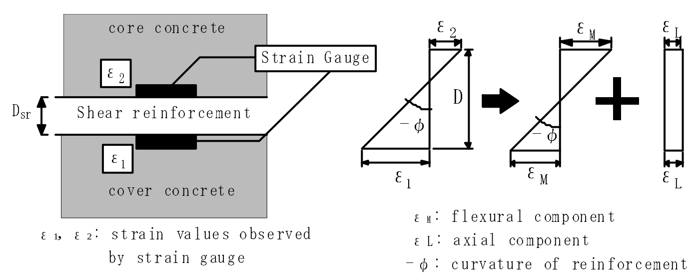

Fig.8 Curvature of shear reinforcement

$$-\phi = \frac{\varepsilon_1 - \varepsilon_2}{D_{sr}} \tag{4}$$

$$\varepsilon_L = \frac{\varepsilon_1 + \varepsilon_2}{2} \tag{5}$$

where ε_1, ε_2 are the values measured by strain gauges, D_{sr} is the diameter of shear reinforcement. Assuming that all 4 sides of the shear reinforcement are simple elastic beams and uniformly loaded as shown in Fig.9(a), the distributions of both bending moment and deflection can be expressed as Fig.9(b) and (c). The expanding areas ($A_{\varphi b}$ related to beam width and $A_{\varphi j}$ related to beam depth in Fig.9(d)) are given by the following equations.

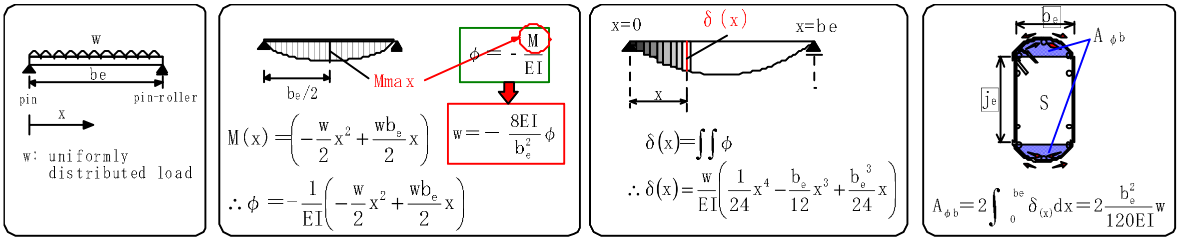

(a) Modeling on side of shear reinforcement (b) Distribution of bending moment (c) Distribution of deflection (d) Expanding area by bending

Fig.9 The increased area by bending

$$A_{\phi b} = 2\frac{b_e^5}{120EI}w \quad (6)$$

$$A_{\phi j} = 2\frac{j_e^5}{120EI}w \quad (7)$$

where E is the modulus of elasticity, and I is geometrical moment of inertia of shear reinforcement. The expanding areas by axial elongation ($A_{\varepsilon b}$ related to beam width, $A_{\varepsilon j}$ related to beam depth in Fig.10) are given by Eq.(8),(9).

$$A_{\varepsilon b} = \varepsilon_{be} \cdot j_e \cdot b_e \quad (8)$$

$$A_{\varepsilon j} = \varepsilon_{je} \cdot j_e \cdot b_e \quad (9)$$

The increment of sectional area consists of four components as shown in Fig.11, which is expressed as the incremental ratio β (%) after all given by Eq.(10) in this paper.

$$\beta = \frac{A_{\phi b} + A_{\varepsilon b} + A_{\phi j} + A_{\varepsilon j}}{S} \times 100 \quad (10)$$

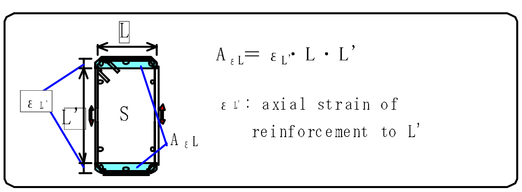

Fig.10 Expanding area by axial

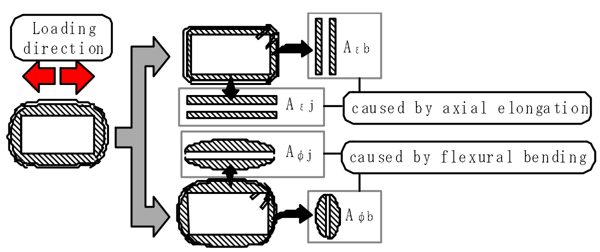

Fig.11 Four components of increased area

Fig.12 shows the relationship between the incremental ratio of core concrete β and drift angle R, where selected core sections are taken as the most deformed part in each specimen. Just before the strength degrading point, β increases extremely. This result suggests that the deterioration of beam shear strength follows after the extreme increase of concrete sectional area. Fig.13 shows the contribution of four components of β on the increase of sectional area. It is said that the expanding deformation by flexural bending of shear reinforcement is much larger than that by axial elongation.

Then, it is thought that the flexural increase by bending of shear reinforcement is the main reason of the shear strength deterioration.

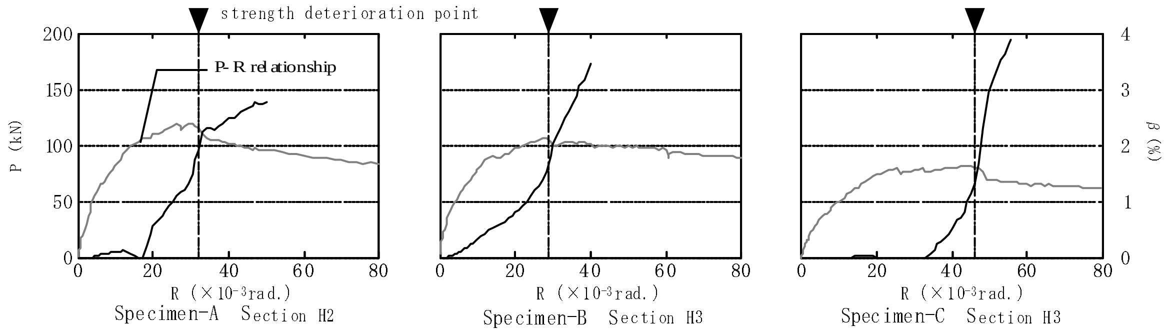

Fig.12 β-R relationship

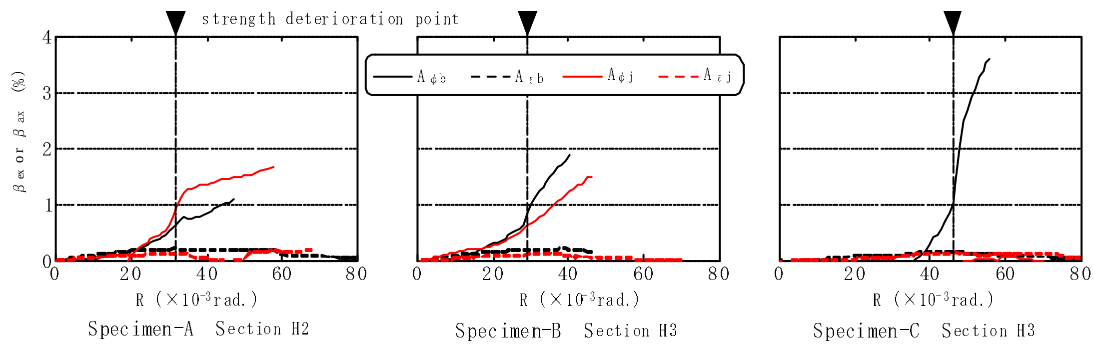

Fig.13 Increment of sectional area by flexural bending and axial elongation

SHEAR BENDING CYCLIC TESTS

Outline

Specimen-D is same as specimen-A except for loading history. The specimen-D was loaded with 2cycles for each drift angle, $\pm5\times10^{-3}$rad., $\pm10\times10^{-3}$rad., $\pm20\times10^{-3}$rad., $\pm40\times10^{-3}$rad., $\pm80\times10^{-3}$rad..

Result and investigation

The observed load P- drift angle R relationships for two specimen-A, D are shown in Fig.14. The shear strength of specimens-D is the same as that of specimen-A, and the envelope curve of specimen-D nearly overlaps the skeleton curve of specimen-A. It is said that these loading history does not affect much on P-R relationship of specimen-D.

Fig.15 shows the expanding area by flexural bending of both specimen-D and specimen-A. In the case of beam which fails in shear, the envelope curve of specimen-D has mutual relationship with the curve of specimen-A, and Therefore the deformations of core concrete under reversed cyclic loading can be

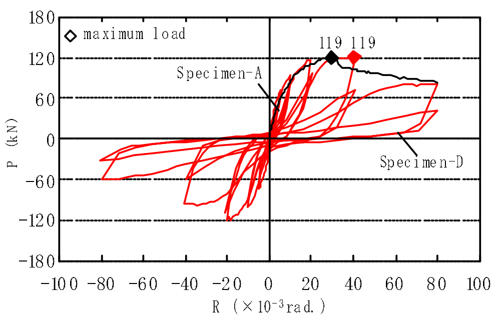

Fig.14 P-R relationship

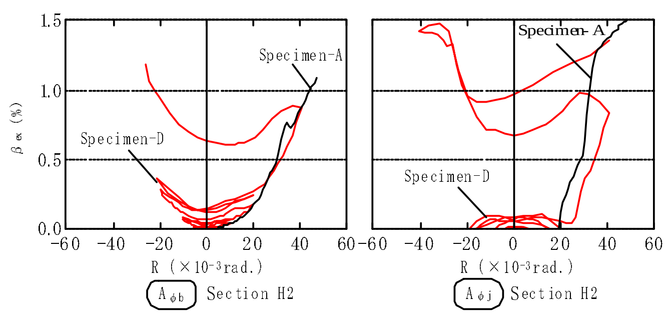

Fig.15 Expanding area by flexural bending

estimated by those under monotonic loading. Specimen-D has residual deformation due to internal cracking when a load becomes zero, and internal damage is accumulated as drift angle increases.

PROPOSAL FOR THE NEW SHEAR FAILURE MECHANISM

As a result of two above mentioned experiments, the following knowledges were obtained to propose a new shear failure mechanism.
1. Truss model includes the stress which affects on the expanding deformation of core concrete.
2. Expanding deformation of core concrete causes the deterioration of shear strength.
3. Deformation of core concrete under cyclic loading can be estimated by those under monotonic loading.
These knowledges show the importance of deformation of core concrete in shear failure mechanism, and then the new concept of shear failure mechanism is proposed as shown in Fig.16.

(1) When loading starts, truss-strut is formed and the stress Pt which is the component of concrete strut as indicated in Fig.1(c) is carried well in the core concrete.
(2) When cracks occur in the core concrete, the parts of core concrete become to move easily. It is thought that the core concrete is moved to the direction of arrows shown in Fig16(2), and the curvature of shear reinforcement increases. At this point, truss-strut keeps forming up to the ultimate limit.

(3) When the drift angle of member increases, the more cracks develop. The truss-strut reaches the unstable state caused by expanding deformation of core concrete at this point, when the strength deterioration starts.

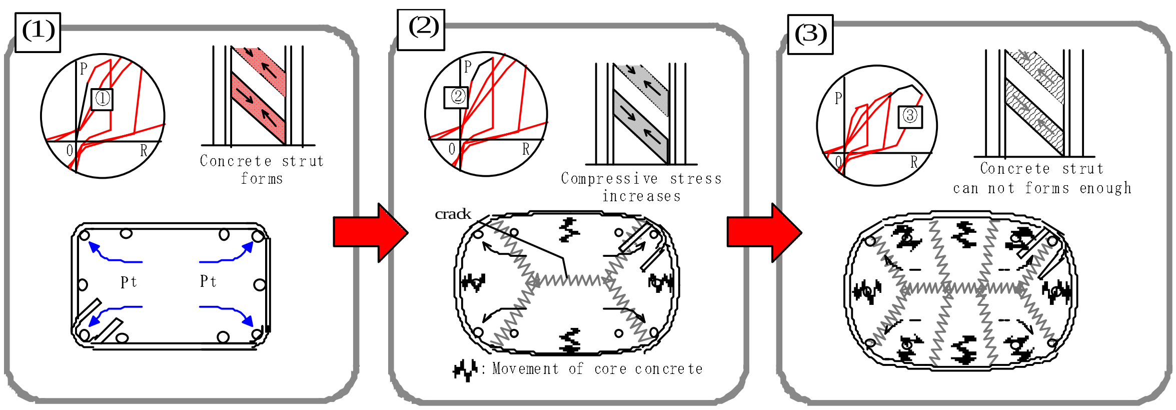

Fig.16 New concept of shear failure mechanism

SHEAR BENDING MONOTONIC LOADING TESTS ON SPECIMENS WITH DIFFERENT SHEAR REINFORCEMENT BAR SECTIONS

Outline

The detail of specimens-E, F, and G are shown in Fig.17, and material properties are listed in Table 3. The test setup, the point where the strain gauges are attached are shown in Fig.4, Fig.5, and all specimens were tested under monotonic loading. The details of these specimens are same as those of specimen-A, except for parameters on the shape of shear reinforcement bar section. Therefore all specimens are designed to initiate shear failure which is caused by compressive failure of core concrete, expressed in AIJ guidelines [1]. The sectional areas and material properties of shear reinforcement are same, but the shape of section is different. The shear reinforcement of specimen-E has the section of normal type(round), that of specimen-F,G have the rectangular section. The shear reinforcement of three types have different geometrical moment of inertia I ($I_E : I_F : I_G = 2 : 4 : 1$), but same sectional area.

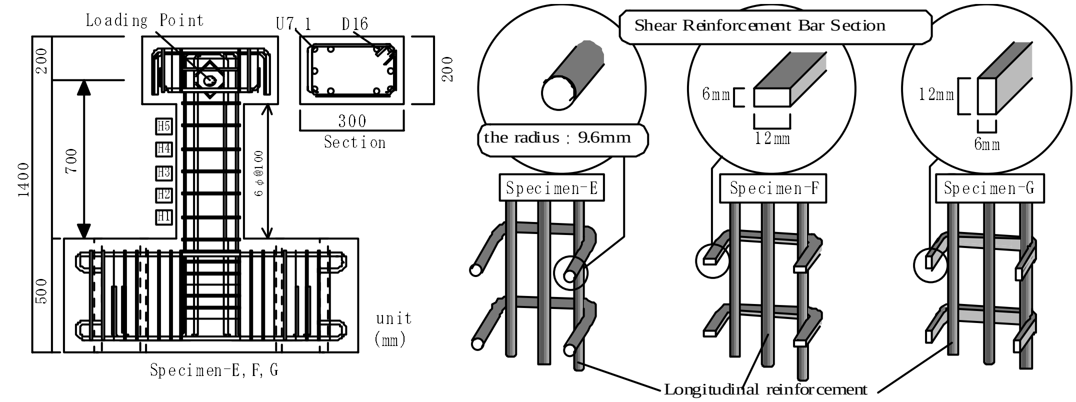

Fig.17 Reinforcement details

Table 3 Material properties

(a) Steel

	Yield Strength (N/mm^2)	Yield Strain ($\times 10^{-6}$)	Young's Modulus (N/mm^2)
Specimen-E	814	4451	2.10×10^5
Specimen-F	796	4078	2.12×10^5
Specimen-G	728	3841	2.13×10^5

(b) Concrete

Specimen	A	B	C
Concrete Strength (N/mm^2)	19.2	19.6	20.3

Result and investigation

The observed load P- drift angle R relationships for three specimens are shown in Fig.18, and the comparison of experimental values with calculation ones (Eq.(2)) are listed in Table 4. The test result shows that the maximum strength of specimen-F is the highest, that of specimen-G is the second, and that of specimen-E is the lowest. The maximum strength of specimen-F exceeds calculation one by about 20%. But the true shear strength might be higher than maximum strength observed, since the some longitudinal bar yielded at the point of 55×10^{-3}rad. which is before the drift angle at maximum strength. Both Specimen-E and G failed in shear without shear reinforcement yielding. According to the AIJ guidelines [1], these three specimens have the same shear strength since there is no parameter on the shape of shear reinforcing bar. But the experiment shows the different results. It is said that the shape of shear reinforcement (moment inertia, round or rectangular) affects on the shear strength of these specimen types.

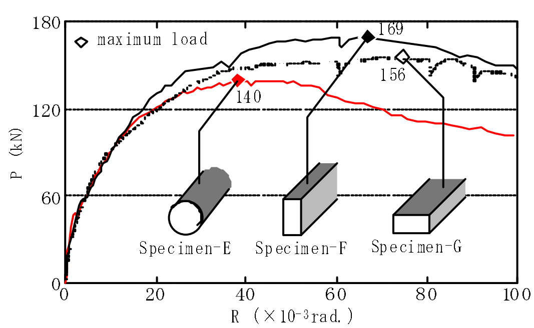

Fig.18 P-R relationship

Table 4 Comparison of maximum strength to

Specimen		E	F	G
Maximum strength (kN)	V_{max}	139.6	169.3	155.7
Calculation Values (kN)	V_{cal}	144.4	143.8	146.2
V_{max}/V_{cal}		0.97	1.18	1.06

The incremental ratios of expanding areas by bending ($\beta_{\varphi b}$ related to beam width, $\beta_{\varphi j}$ related to beam depth) are calculated by Eq.11, 12.

$$\beta_{\phi b} = \frac{A_{\phi b}}{S} \times 100 \tag{11}$$

$$\beta_{\phi j} = \frac{A_{\phi j}}{S} \times 100 \tag{12}$$

Fig.19 shows only $\beta_{\varphi b}$ and $\beta_{\varphi j}$ of specimen-E, F, G, because the expanding areas by axial elongation hardly increased. The figure shows that expanding deformation of specimen-F, G are controlled by shear reinforcement which have the rectangular section.

As a result, it is confirmed that control of expanding deformation of core concrete effects on the improvement of shear strength, and when sectional area of stirrup are same, rectangular stirrup has higher confined effect than round one.

The relationship between expanding deformation of core concrete and the strength deterioration point for all six specimens are shown in Fig.20. The figure indicates that the strength deterioration of all specimens starts when the value of β reaches to about 2%.

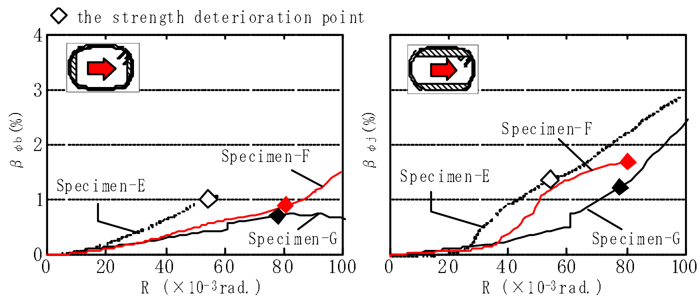

Fig.19 Expanding deformation of core concrete

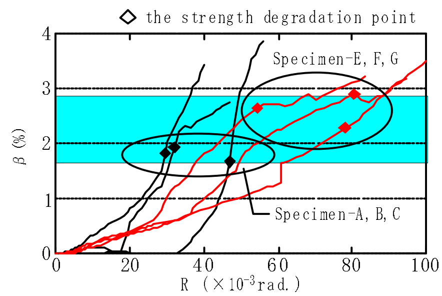

Fig.20 Relationship between deformation of core concrete and the drift angle R at shear strength deterioration point for all specimens

CONCLUSION

Based on the experimental tests results, new shear resistant mechanism to RC beam with sufficient shear reinforcement is proposed by quantifying the expansion behavior of core concrete, and the conclusions are as follows.

1. Truss model includes the stress which affects on the expanding deformation of core concrete.
2. Deformations of core concrete under cyclic loading can be estimated by those under monotonic loading.
3. Expanding deformation of core concrete causes the deterioration of shear resistant mechanism.
4. Control of expanding deformation by flexural bending of core concrete effects on the improvement of shear strength.
5. When some sectional area of core concrete increases to about 2%, shear strength starts to deteriorate.
6. When sectional areas of stirrup are same, and the rectangular stirrup with larger geometrical moment inertia have higher confined effect than round one.

REFERENCES

1. Architectural Institute of Japan(1999) "Design Guidelines for Earthquake Resistant Reinforced Concrete Buildings Based on Inelastic Displacement Concept" (in Japanese)
2. Tsurui, M. Arai, D. Mukai, T. and Nomura, S.(2000) "Experimental Study on Shear Characteristics of RC Beams with High Tension Shear Reinforcement" Summaries of Technical Papers of Annual Meeting Architectural Institute of Japan (in Japanese)
3. Ichinose, T.(2001) "Three Dimensional Shear Failure of RC Columns after Cyclic Loading" Committee Report, American Society of Civil Engineers, pp.546-561